*Supporting Information*

# Mussel-Inspired Injectable Hydrogel Adhesive Formed under Mild Conditions Features Near-Native Tissue Properties

Kongchang Wei,[1,#] Berna Senturk,[2,#] Martin T. Matter,[3,4,5] Xi Wu,[6] Inge K. Herrmann,[3,4] Markus Rottmar,[2,*] Claudio Toncelli[1,*]

*[1]Laboratory for Biomimetic Membranes and Textiles, [2]Laboratory for Biointerfaces,[3] Laboratory for Particles-Biology Interactions, Empa, Swiss Federal Laboratories for Materials Science and Technology, Lerchenfeldstrasse 5, 9014 St. Gallen, Switzerland; [4]Nanoparticle Systems Engineering Laboratory, Institute of Process Engineering, Department of Mechanical and Process Engineering, [5]Particle Technology Laboratory, Institute of Process Engineering, Department of Mechanical and Process Engineering, ETH Zurich, Sonneggstrasse 3, 8092 Zurich, Switzerland; [6]Institute for Mechanical Systems, ETH Zürich, Leonhardstrasse 21, 8092 Zürich Switzerland.*

*# equal contribution*

** corresponding authors, markus.rottmar@empa.ch; claudio.toncelli@empa.ch*

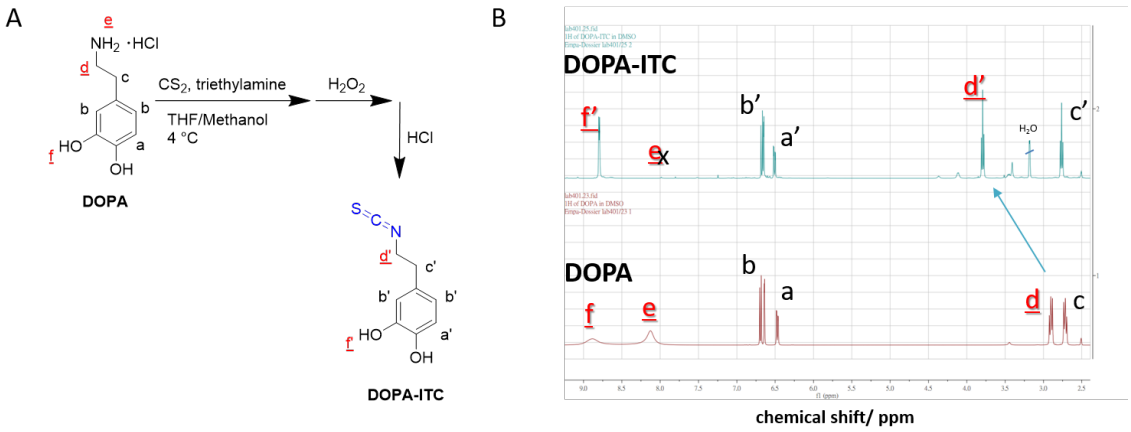


**Figure S1.** (A) The synthetic rout of DOPA-ITC. (B) $^{1}$H NMR characterization of DOPA-ITC (in DMSO-*d6*) and DOPA. The successful conversion of the primary amine group into isothiocyanate (ITC) group is evidenced by the shifting of signal *d* to *d'*, the disappearance of signal *e* and the sharpening of signal *f*.

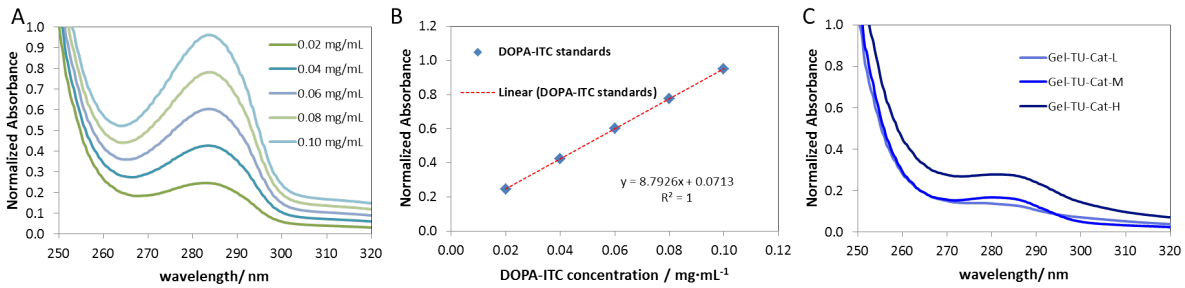


**Figure S2.** (A) Representative UV-vis spectra of DOPA-ITC in the presence of gelatin (1 mg/mL) for the standard curve. (B) Standard curve of DOPA-ITC absorbance (n = 3, as given in Table S1). (C) Representative UV-vis spectra of Gel-TU-Cat (1 mg/mL), with absorbance at 282 nm (n = 3) given in Table S2.

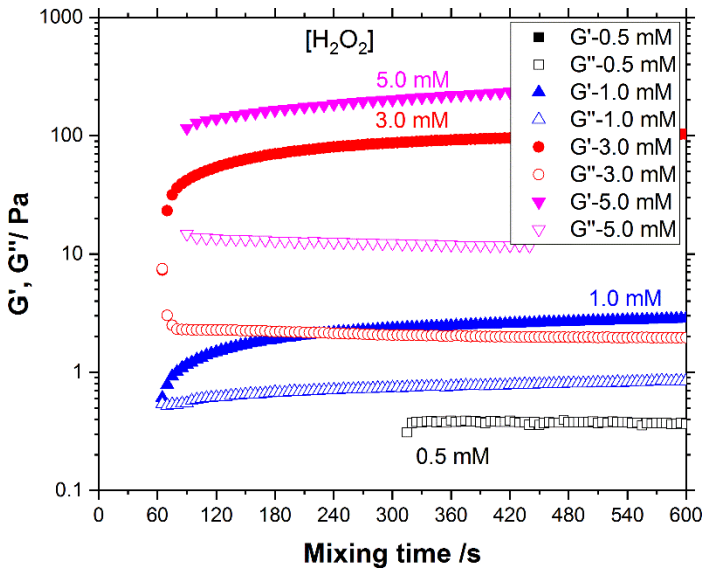


**Figure S3.** Gelation of Gel-TU-Cat-M polymer triggered by $H_2O_2$ at different concentration characterized by rheological time sweep measurement (HRP 5 units/mL).

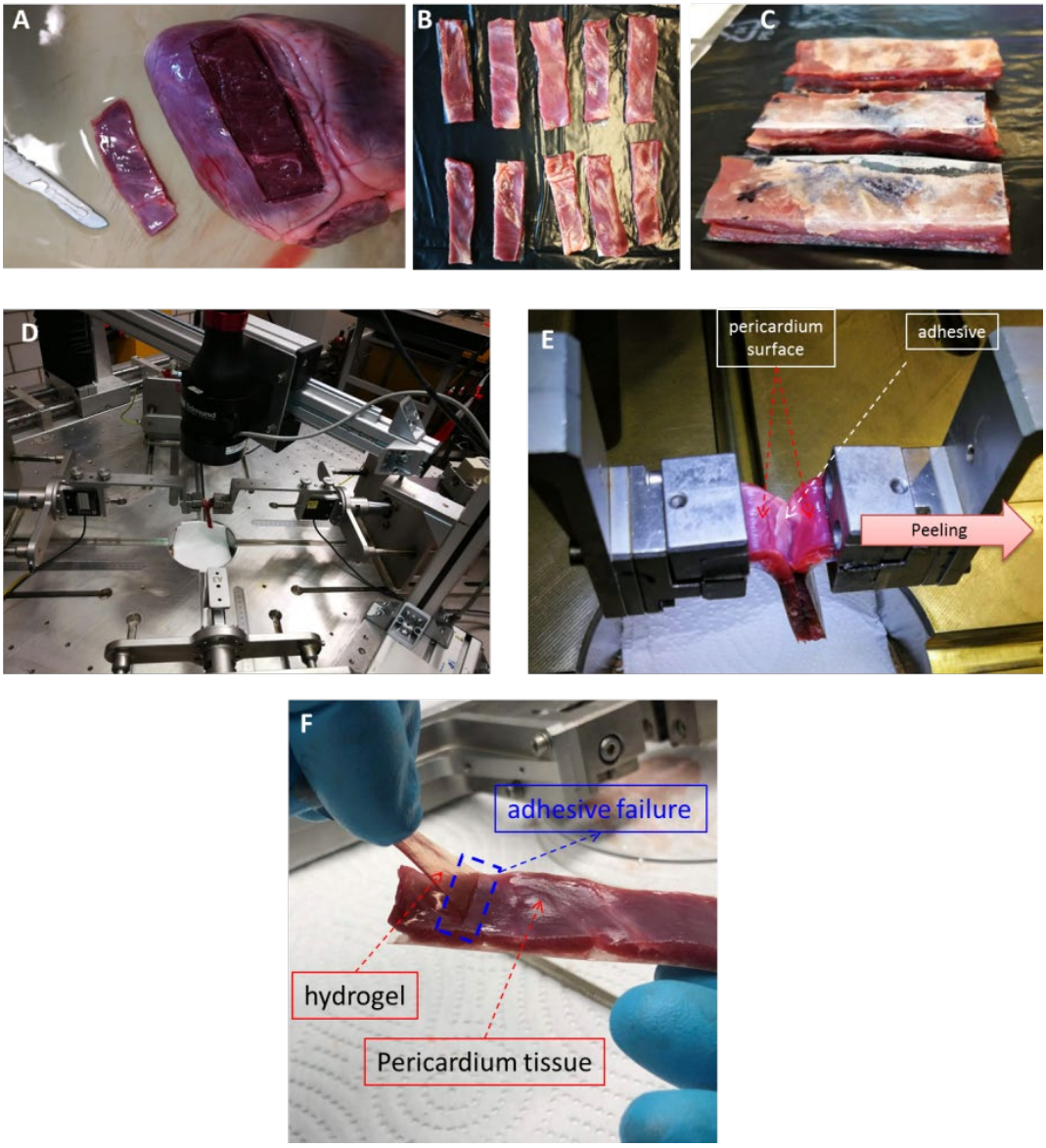


**Figure S4.** Schematic illustration of the T-peeling tests according to the ASTM F2256-05 standard protocol. (A) A piece of rectangular pericardium tissue was carefully peeled off from a fresh porcine heart. (B) The raw tissue specimens were backed by PET films with Superglue on the cut surface, leaving the original heart tissue surface blank. (C) The test specimens with two pieces of PET-backed pericardium tissues glued with hydrogels as described in panel D. (D-E) Digital images of the horizontal T-peeling setup. (F) A representative specimen with a piece of hydrogel being manually peeled off from the tissue surface, adhesive failure was observed instead of cohesive failure.

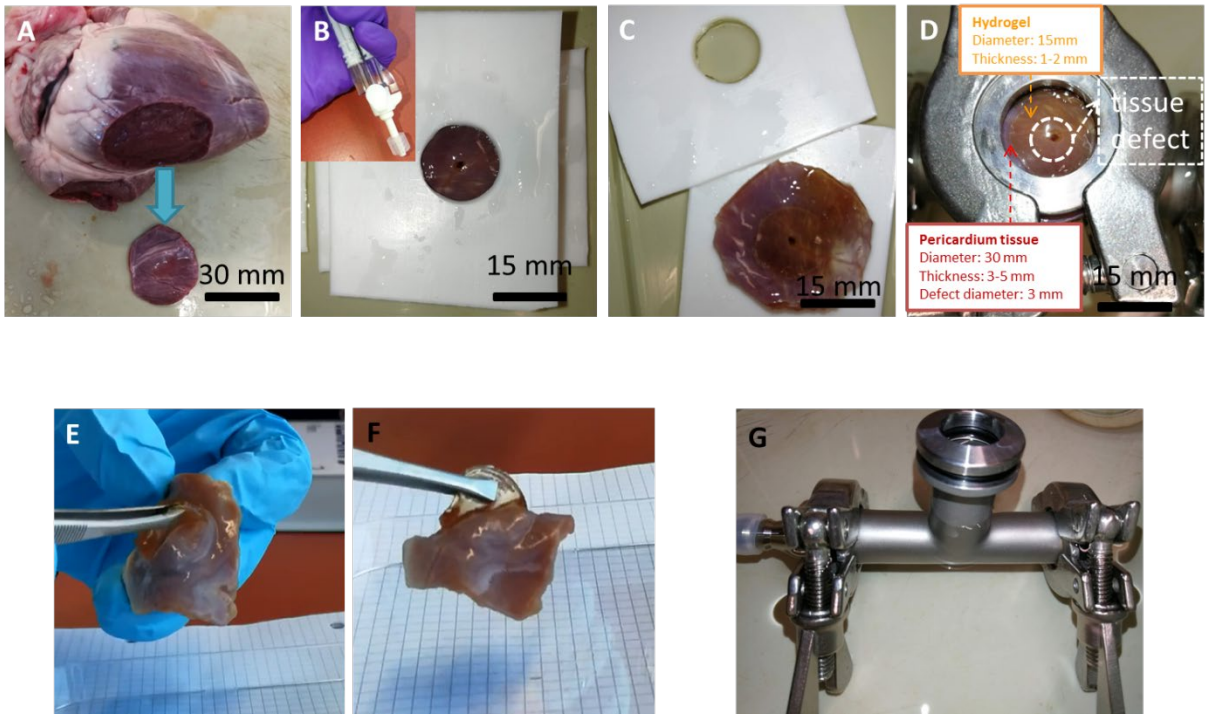


**Figure S5.** Schematic illustration of the bursting strength measurement according to the ASTM F2392 standard. (A) A piece of pericardium tissue was carefully peeled off from a fresh porcine heart. (B) The formation of hydrogel adhesives on the pericardium tissues with penetrating defects. (C) A piece of hydrogel-sealed pericardium tissue for bursting test. (D) The fixed specimen on the testing chamber. (E) A piece of testing specimen after burst showing the adhesive failure on one part of the interface. (F) The residual adhesion after burst remains strong enough to lift up the tissue. (G) A digital image of the testing chamber.

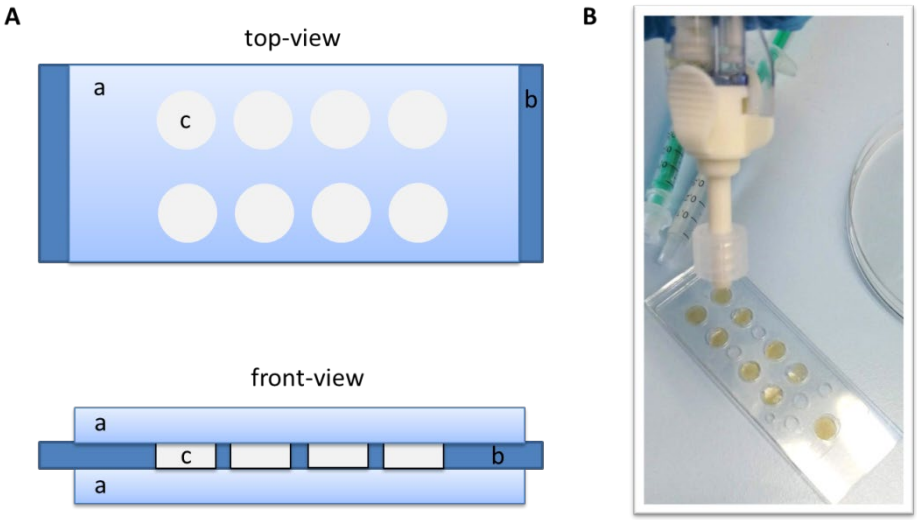


**Figure S6.** Schematic top-view and front-view illustration (A) and a digital image (B) of the experimental setup for preparation of cell-laden hydrogel disk (a: Glass slides pre-treated with Sigmacote agents; b: PDMS mold with 1 mm thickness; c: Circular holes with 6 mm in diameter and 1mm in thickness).

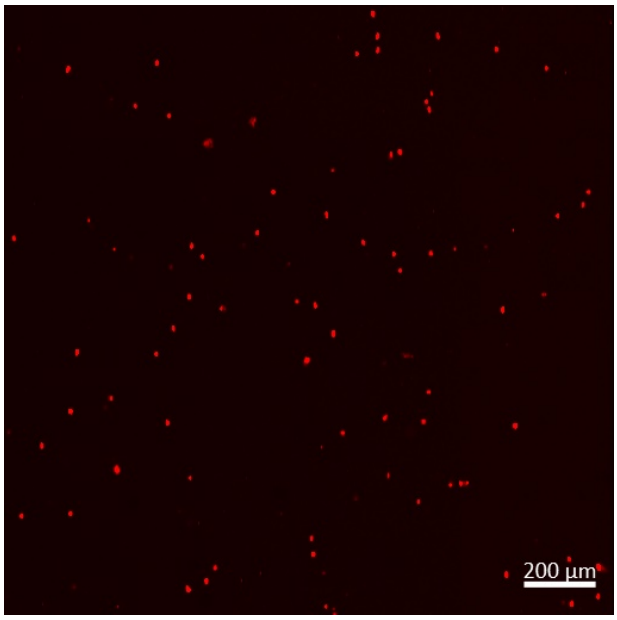


**Figure S7.** Dead cell control of the live/dead staining assay. Live/dead staining of normal human dermal fibroblasts (NHDFs) cultivated in 3D Gel-TU-Cat-M hydrogel matrix and treated with digitonin for 5 min.

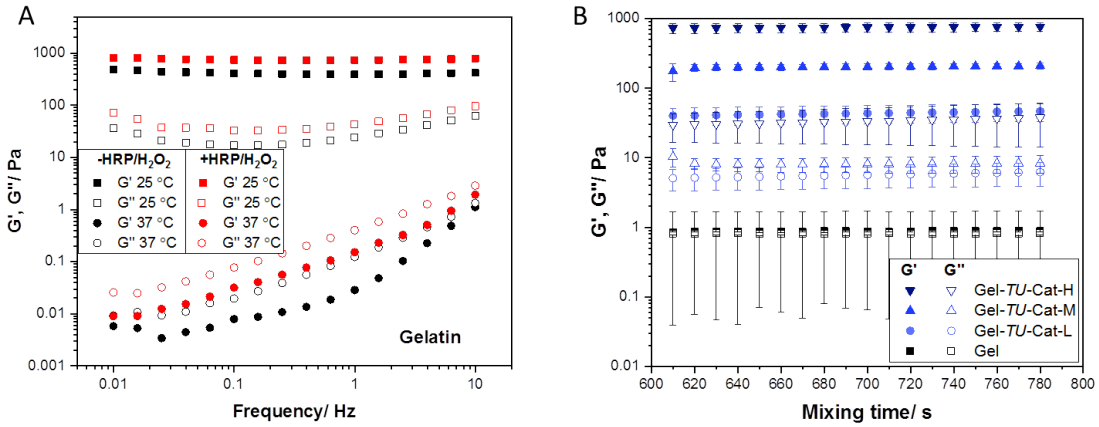


**Figure S8.** (A) Rheological frequency sweep measurements of gelatin solution (100 mg/mL) before or after treatment with enzymatic oxidation (HRP 5 units/mL, $H_2O_2$ 5 mM). The preserved thermo-responsive sol-gel transition indicates that negligible chemical alteration of the gelatin polymer backbone was caused by the enzymatic oxidation. (B) Dynamic oscillatory time sweep rheological measurements of gelatin or Gel-TU-Cat hydrogels started at 10 min after being prepared directly on the rheometer sample plate. The steady modulus (G' and G'') of all the Gel-TU-Cat hydrogels indicate that the gelation process has finished before the measurements were started. In contrast, the gelatin solution under the same crosslinking condition was still in liquid state.

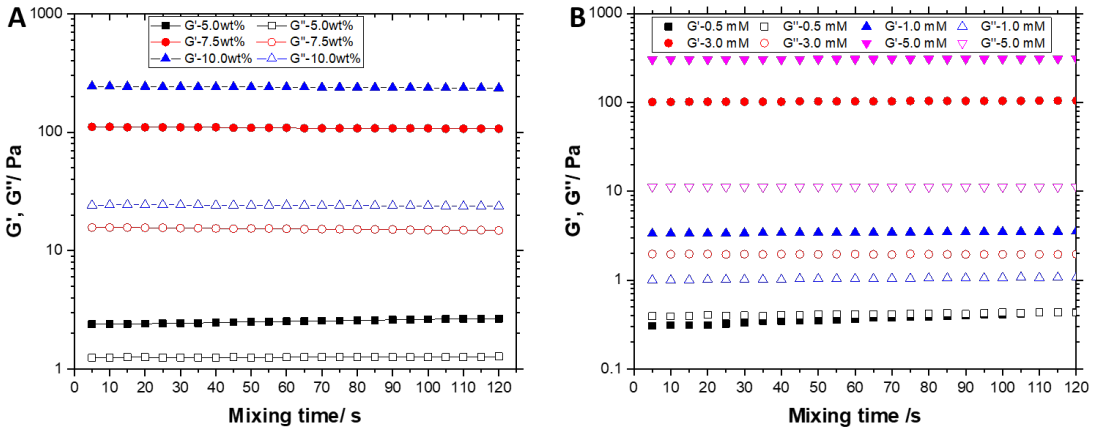


**Figure S9.** Influence of (A) Gel-TU-Cat-M polymer concentration and (B) $H_2O_2$ concentration on hydrogel mechanical properties characterized by rheological time sweep measurement (HRP 5 units/mL). The measurements started 30 minutes after the hydrogels were injected on the sample plate of the rheometer.

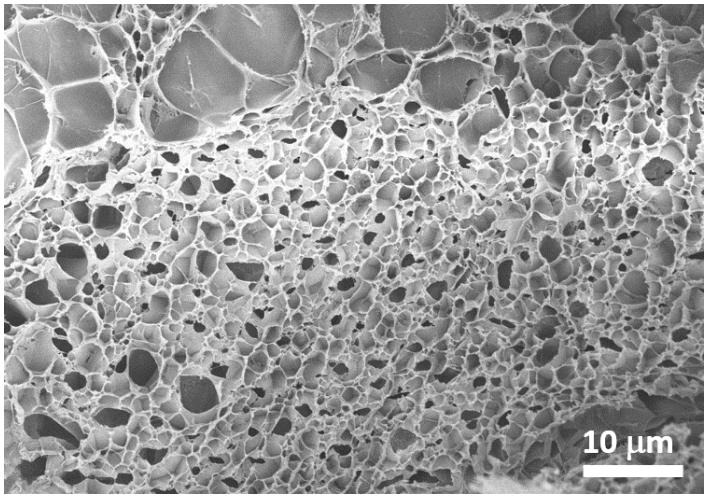


**Figure S10.** SEM images showing the more homogenous structure of the Gel-TU-Cat-H hydrogel formed with lower HRP (1 unit/mL) and $H_2O_2$ (1 mM) concentrations.

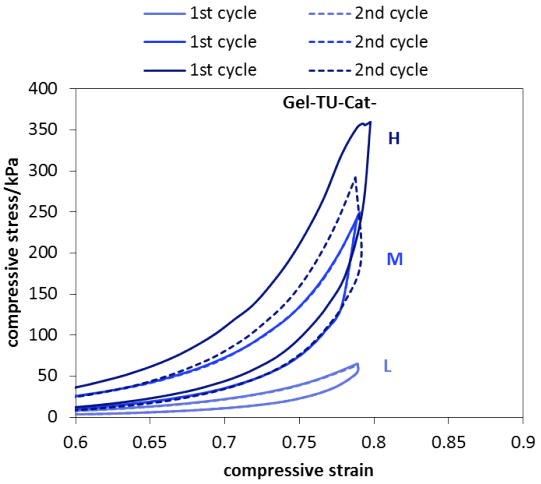


**Figure S11.** Two consecutive loading-unloading compressive cycles with the enlarged strain range of 0.6-0.9, showing the nearly identical hysteresis loops between the first and second cycles of Gel-TU-Cat-L and Gel-TU-Cat-M hydrogels. However, for Gel-TU-Cat-H hydrogels with higher chemical crosslinking densities, in addition to the temporal dissociation of sacrificial non-covalent bonds, partial disruption of the chemical crosslinks occurred during the first cycle, thus leading to the compromised mechanical strength as shown in the second cycle.

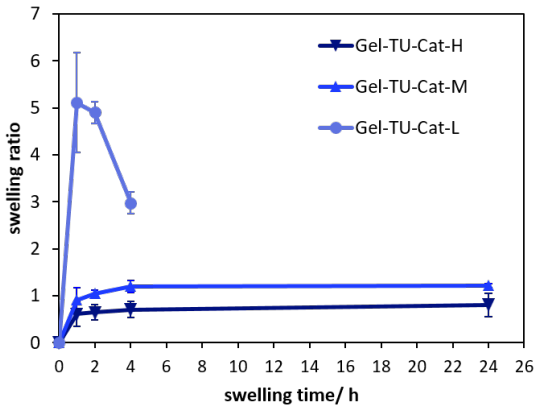


**Figure S12.** Swelling test of Gel-TU-Cat hydrogels in PBS at 37 °C. The swelling ratio was calculated by $(W_t - W_0)/W_0$, where $W_t$ is the hydrogel weight at a certain swelling time point (t), and $W_0$ is the initial hydrogel weight before swelling. A clear weight loss of the Gel-TU-Cat-L hydrogels after 2 hours of swelling indicates its poorer stability than that of the Gel-TU-Cat-M and Gel-TU-Cat-H hydrogels.

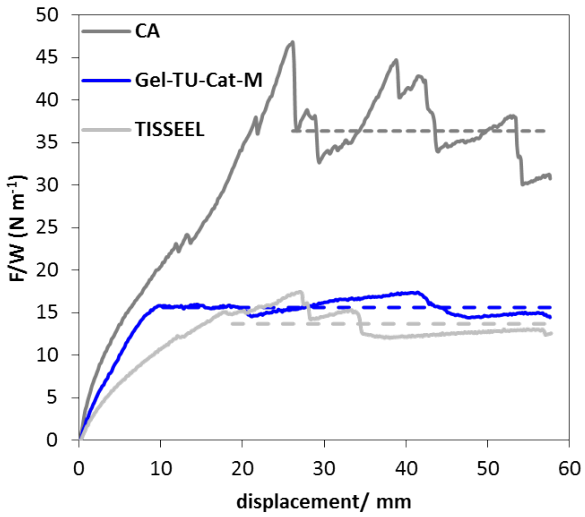


**Figure S13.** Representative peeling curves of CA, Gel-TU-Cat-M and TISSEEL fibrin glues on pericardium tissue surfaces with the averaged plateau value (dash lines) plotted. The huge fluctuation of the peeling curve indicates the existence of significant interfacial inhomogeneity between solidified CA adhesives and the tissues surfaces.

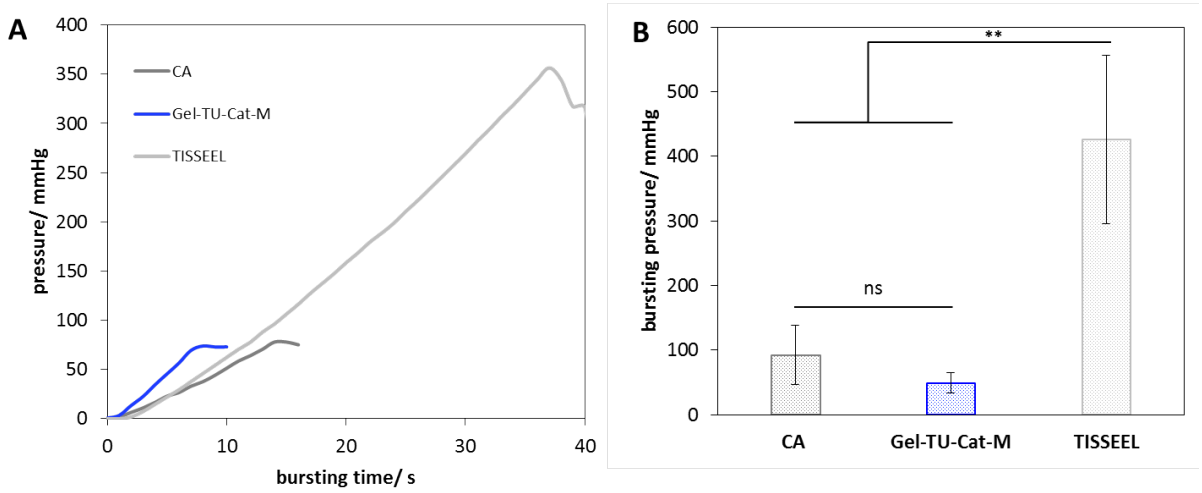


**Figure S14.** Representative bursting curves (A) and averaged bursting strength (B) of different adhesives on porcine pericardium tissues in PBS at 37 °C. Before every measurement, the whole burst test setup was immersed in a 37 °C PBS bath for 15 minutes (n = 4, **p < 0.01, ns for non-significant difference).

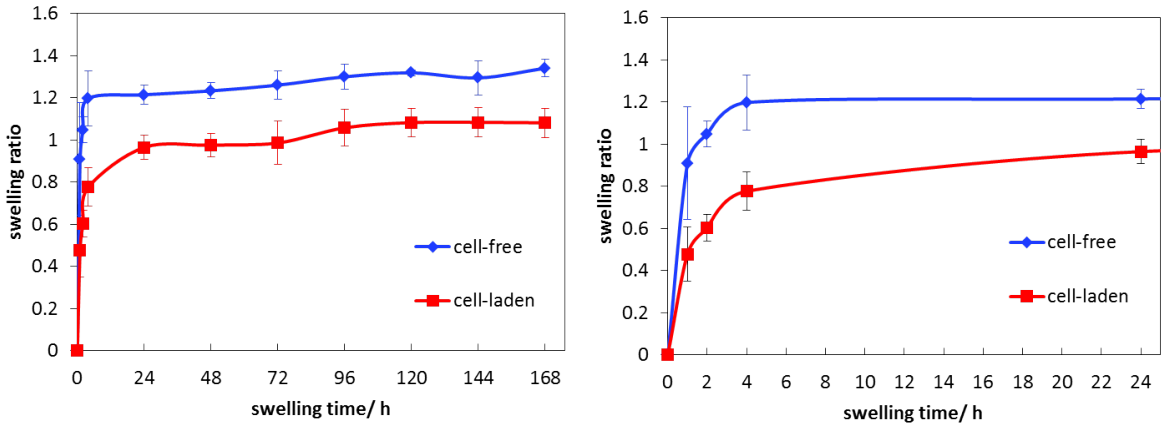


**Figure S15.** Swelling behaviors of cell-free Gel-TU-Cat-M hydrogels in PBS and cell-laden Gel-TU-Cat-M hydrogels in culture medium at 37 °C. The swelling ratio was calculated by $(W_t - W_0)/W_0$, where $W_t$ is the hydrogel weight at a certain swelling time point (t), and $W_0$ is the initial hydrogel weight before swelling.

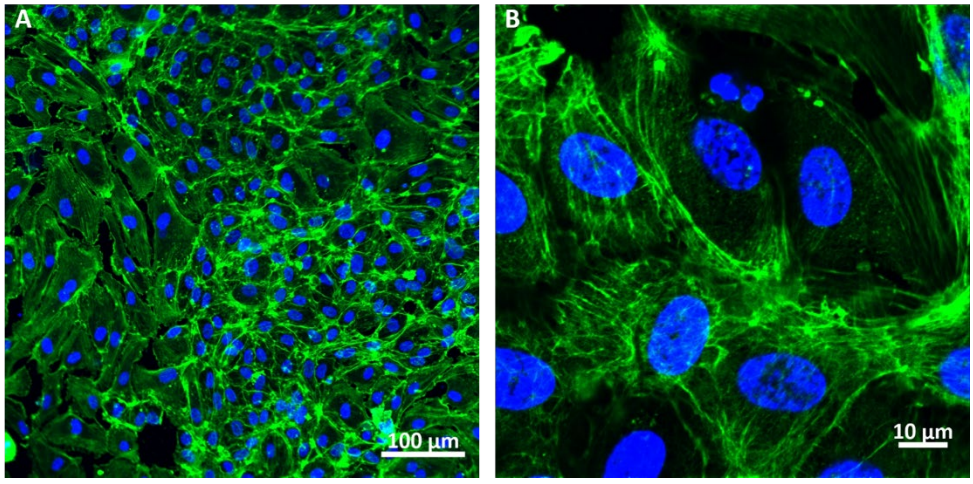


**Figure S16**. Confocal images human umbilical vein endothelial cells (HUVECs) cultivated on 2D Gel-TU-Cat-M hydrogel surface for 7 days after staining of F-actin filaments (green) and cell nuclei (blue), with both (A) low and (B) high magnification.

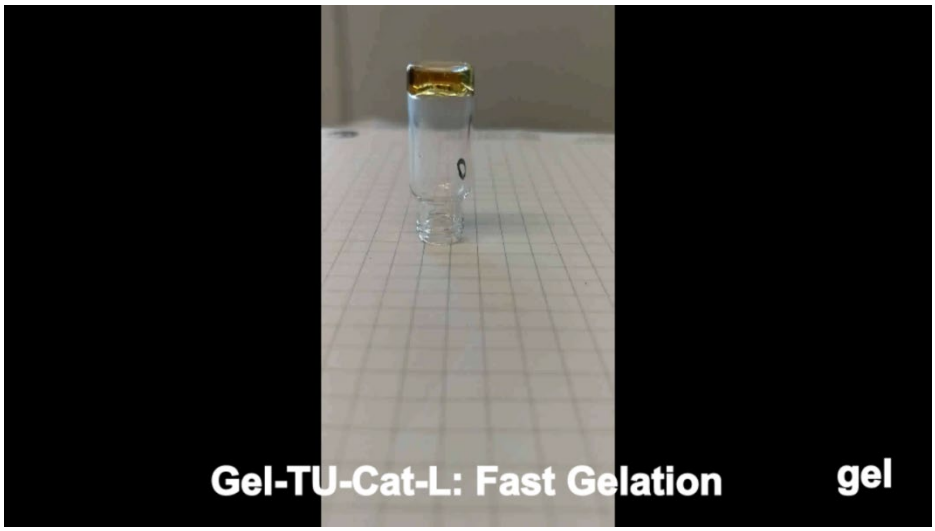


**Movie S1.** The tube inversion test revealing the fast gelation of Gel-TU-Cat-L (The hydrogel was prepared with a double syringe biomaterial delivery K-system as described in the main text Section 2.5).

**Supplementary Note 1: Fitting the stress relaxation data to the Maxwell-Weichert model.**

The stress relaxation data for the Gel-TU-Cat hydrogels were fit to a Maxwell-Weichert model with 2 Maxwell elements in parallel (Figure 3D). Good fits were obtained with double exponential decay (ExpDecay2 function from Origin 2018, Equation S1) and the best-fit parameters are shown in Table S3.

$$Y = Y_0 + A_1Exp(-t/\tau_1) + A_2Exp(-t/\tau_2) \quad \text{(Equation S1)}$$

**Supplementary Note 2: Calculation of Young's modulus.**

The Young's modulus (E) of Gel-TU-Cat hydrogels was calculated from the linear fitting of the initial part of the compressive stress-strain curves with strain below 0.25 (Figure 4C), and summarized together with the catechol contents ([Cat] μmol/g polymer) in Figure 4D. The fitting parameters are shown in Table S4.

**Supplementary Note 3: Catechol content of PEG-DOPAs from reference #29.**

Among all PEG-DOPAs Polymers investigated in this referene, polymer **I** has the fastest gelation (in 2 minutes). According to "**Table 1.** Molecular Weight and Coupling Efficiency of DOPA-Modified PEGs" reported in the paper, the molecular weight of the polymer **I** PEG-$(DOPA)_4$ is 11900 Da, the "%DOPA coupling efficiency" is 85.3%. Therefore, the catechol content of this polymer is:

$$4 \times 85.3\% \div 11900 = 2.867 \times 10^{-4}\ mol/g = 286.7\ \mu mol/g$$

**Table S1.** Normalized absorbance (at 282 nm) of DOPA-ITC standard solutions (n = 3) in the presence of gelatin (1 mg/mL).

| Concentration | Normalized Absorbance at 282 nm | | | |
|---|---|---|---|---|
| mg/mL | 1 | 2 | 3 | Mean ±SD |
| 0.02 | 0.2458 | 0.2441 | 0.2455 | 0.2451 ± 0.0007 |
| 0.04 | 0.4240 | 0.4230 | 0.4254 | 0.4241 ± 0.0010 |
| 0.06 | 0.5987 | 0.6000 | 0.6034 | 0.6007 ± 0.0020 |
| 0.08 | 0.7733 | 0.7817 | 0.7732 | 0.7761 ± 0.0040 |
| 0.10 | 0.9520 | 0.9453 | 0.9478 | 0.9484 ± 0.0028 |

**Table S2.** Normalized absorbance (at 282 nm) of Gel-TU-Cat solutions (1 mg/mL, n = 3).

| | **Normalized Absorbance at 282 nm** | | | |
|---|---|---|---|---|
| | 1 | 2 | 3 | Mean ± SD |
| Gel-TU-Cat-L | 0.1341 | 0.1327 | 0.1349 | 0.1339 ± 0.0009 |
| Gel-TU-Cat-M | 0.1660 | 0.1659 | 0.1662 | 0.1660 ± 0.0001 |
| Gel-TU-Cat-H | 0.2782 | 0.2786 | 0.2792 | 0.2786 ± 0.0004 |

**Table S3.** Best-fit parameters of the Gel-TU-Cat-M hydrogel stress relaxation obtained with double exponential decay (ExpDecay2 function from Origin 2018, Equation S1).

| **strain/ %** | **$\tau_1$/s** | **$\tau_2$/s** | **R-square** |
|---|---|---|---|
| 10 | 6.68 | 410.02 | 0.9768 |
| 30 | 8.13 | 422.67 | 0.9911 |
| 50 | 6.05 | 352.26 | 0.9917 |
| 70 | 6.18 | 344.48 | 0.9933 |
| 90 | 5.24 | 292.92 | 0.9932 |
| Mean ± SD | 6.46 ± 0.96 | 364.47± 47.18 | 0.9892± 0.0063 |

**Table S4.** Fitting parameters of the initial part of the compressive stress-strain curves with strain below 0.25 (n = 3).

| | **Linear fitting** | | | | | | **Analysis of Young's Modulus** | | | | | |
|---|---|---|---|---|---|---|---|---|---|---|---|---|
| | 1 | | 2 | | 3 | | E/ kPa | | | | *P* value | |
| | Slope | $R^2$ | Slope | $R^2$ | Slope | $R^2$ | 1 | 2 | 3 | Mean ± SD | *vs.* Gel-TU-Cat-L | *vs.* Gel-TU-Cat-H |
| **Gel-TU-Cat-L** | 4368 | 0.9957 | 3253 | 0.9826 | 3456 | 0.9942 | 4.4 | 3.3 | 3.5 | 3.7 ± 0.5 | x | 0.0004 |
| **Gel-TU-Cat-M** | 10402 | 0.9779 | 12125 | 0.9700 | 9068 | 0.9822 | 10.4 | 12.1 | 9.1 | 10.5 ± 1.2 | 0.0020 | 0.0104 |
| **Gel-TU-Cat-H** | 19587 | 0.9904 | 16031 | 0.9688 | 16080 | 0.9769 | 19.6 | 16.0 | 16.1 | 17.2 ± 1.7 | 0.0004 | x |

**Table S5.** Statistical analysis of T-Peeling data (n = 4).

| | **adhesion energy/ J $m^{-2}$** | | | | | ***P* Value** | |
|---|---|---|---|---|---|---|---|
| | 1 | 2 | 3 | 4 | Mean ± SD | *vs.* CA | *vs.* TISSEEL |
| **CA** | 48.30 | 74.53 | 72.75 | 48.04 | 60.90 ± 12.75 | x | 0.0048 |
| **Gel-TU-Cat-M** | 24.76 | 26.76 | 25.61 | 31.25 | 27.09 ± 2.50 | 0.0041 | 0.6070 |
| **TISSEEL** | 17.14 | 27.38 | 34.20 | 20.94 | 24.92 ± 6.49 | 0.0048 | x |

**Table S6.** Statistical analysis of bursting pressure data (25 °C, n = 10).

| | **Bursting pressure/ mmHg** | | | | | | | | | | | ***P* values** | |
|---|---|---|---|---|---|---|---|---|---|---|---|---|---|
| | 1 | 2 | 3 | 4 | 5 | 6 | 7 | 8 | 9 | 10 | Mean ± SD | vs. CA | vs. TISSEEL |
| CA | 276.68 | 230.87 | 272.10 | 176.82 | 169.49 | 287.67 | 174.98 | 269.35 | 194.22 | 271.18 | 232.34 ± 46.11 | x | $4 \times 10^{-9}$ |
| Gel-TU-Cat-M | 79.71 | 185.06 | 88.87 | 118.78 | 105.36 | 109.94 | 123.68 | 251.02 | 122.76 | 87.95 | 127.31 ± 49.82 | 0.0002 | 0.0007 |
| TISSEEL | 64.13 | 17.41 | 87.03 | 59.55 | 50.39 | 57.72 | 36.65 | 75.12 | 21.99 | 66.88 | 53.69 ± 21.28 | $4 \times 10^{-9}$ | x |

**Table S7.** Statistical analysis of T-Peeling data (37 °C, n = 4).

| | adhesion energy/ J $m^{-2}$ | | | | | *P* Value | |
|---|---|---|---|---|---|---|---|
| | 1 | 2 | 3 | 4 | Mean ± SD | *vs.* CA | *vs.* TISSEEL |
| **CA** | 76.04 | 168.57 | 77.87 | 47.64 | 92.53 ± 45.51 | x | 0.0058 |
| **Gel-TU-Cat-M** | 73.89 | 44.57 | 48.56 | 29.32 | 49.08 ± 16.02 | 0.1698 | 0.0025 |
| **TISSEEL** | 247.36 | 564.35 | 356.38 | 535.95 | 426.01 ± 130.37 | 0.0058 | x |